Cicirelli, M. F., Pelech, S. L., & Krebs, E. G. (1988) *J. Biol. Chem. 263*, 2009–2019.
Colbran, R. J., Fong, Y.-L., Schworer, C. M., & Soderling, T. R. (1988) *J. Biol. Chem. 263*, 18145–18151.
Colbran, R. J., Schworer, C. M., Hashimoto, Y., Fong, Y.-L., Rich, D. P., Smith, K., & Soderling, T. R. (1989) *Biochem. J. 258*, 313–325.
De Camilli, P., & Greengard, P. (1986) *Biochem. Pharmacol. 35*, 4349–4357.
Eckberg, W. R. (1988) *Biol. Bull. 174*, 95–108.
Fong, Y.-L., Taylor, W. L., Means, A. R., & Soderling, T. R. (1989) *J. Biol. Chem. 264*, 16759–16763.
Fukunaga, K., Goto, S., & Miyamoto, E. (1988) *J. Neurochem. 51*, 1070–1078.
Hanks, S. K., Quinn, A. M., & Hunter, T. (1988) *Science 241*, 42–52.
Hanley, R. M., Means, A. R., Ono, T., Kemp, B. E., Burgin, K. E., Waxham, N., & Kelly, P. T. (1987) *Science 237*, 293–297.
Hanley, R. M., Means, A. R., Kemp, B. E., & Shenolikar, S. (1988) *Biochem. Biophys. Res. Commun. 152*, 122–128.
Hanson, P. I., Kapiloff, M. S., Lou, L. L., Rosenfeld, M. G., & Schulman, H. (1989) *Neuron 3*, 59–70.
Hardie, G. (1988) *Nature 335*, 592–593.
Kaufman, R. J., Davies, M. V., Patchak, V. K., & Hershey, J. W. (1989) *Mol. Cell. Biol. 9*, 946–958.
Kelly, P. T., Weinberger, R. P., & Waxham, M. N. (1988) *Proc. Natl. Acad. Sci. U.S.A. 85*, 4991–4995.
Kunkel, T. A. (1985) *Proc. Natl. Acad. Sci. U.S.A. 82*, 488–492.
Kuret, J., Johnson, K. E., Nicolette, C., & Zoller, M. J. (1988) *J. Biol. Chem. 263*, 9149–9154.
Kwiatkowski, A. P., & King, M. M. (1989) *Biochemistry 28*, 5380–5385.
LeVine, H., III, & Sahyoun, N. E. (1987) *Eur. J. Biochem. 168*, 481–486.
Lin, C. R., Kapiloff, M. S., Durgerian, S., Tatemoto, K., Russo, A. F., Hanson, P., Schulman, H., & Rosenfeld, M. G. (1987) *Proc. Natl. Acad. Sci. U.S.A. 84*, 5962–5966.
Llinas, R., McGuinness, T. L., Leonard, C. S., Sugimori, M., & Greengard, P. (1985) *Proc. Natl. Acad. Sci. U.S.A. 82*, 3035–3039.
Lou, L. L., & Schulman, H. (1989) *J. Neurosci. 9*, 2020–2032.
Malinow, R., Schulman, H., & Tsien, R. W. (1989) *Science 245*, 862–865.
Maurer, R. A. (1989) *J. Biol. Chem. 264*, 6870–6873.
Miller, S. G., Patton, B. L., & Kennedy, M. B. (1988) *Neuron 1*, 593–604.
Muramatsu, M., Kaibuchi, K., & Arai, K. (1989) *Mol. Cell. Biol. 9*, 831–836.
Payne, M. E., Fong, Y.-L., Ono, T., Colbran, R. J., Kemp, B. E., Soderling, T. R., & Means, A. R. (1988) *J. Biol. Chem. 263*, 7190–7195.
Roskoski, R., Jr. (1985) *Methods Enzymol. 99*, 3–6.
Scholz, W. K., Baitinger, C., Schulman, C., & Kelly, P. T. (1988) *J. Neurosci. 8*, 1039–1051.
Schulman, H. (1984) *J. Cell Biol. 99*, 11–19.
Schulman, H. (1988) *Adv. Second Messenger Phosphoprotein Res. 22*, 39–112.
Schulman, H., & Greengard, P. (1978) *Proc. Natl. Acad. Sci. U.S.A. 75*, 5432–5436.
Schulman, H., & Lou, L. L. (1989) *Trends Biochem. Sci. 14*, 62–66.
Schworer, C. M., Colbran, R. J., Keefer, J. R., & Soderling, T. R. (1988) *J. Biol. Chem. 263*, 13486–13489.
Thiel, G., Czernik, A. J., Gorelick, F., Nairn, A. C., & Greengard, P. (1988) *Proc. Natl. Acad. Sci. U.S.A. 85*, 6337–6341.
Thorsness, P. E., & Koshland, D. E., Jr. (1987) *J. Biol. Chem. 262*, 10422–10425.
Zoller, M. J., & Smith, M. (1983) *Methods Enzymol. 100*, 468–500.

Mechanistic Studies of Peptidyl Prolyl Cis–Trans Isomerase: Evidence for Catalysis by Distortion

Richard K. Harrison and Ross L. Stein*
Department of Enzymology, Merck Research Laboratories, P.O. Box 2000, Rahway, New Jersey 07065
Received November 28, 1989; Revised Manuscript Received December 26, 1989

ABSTRACT: Cyclophilin, the cytosolic binding protein for the immunosuppressive drug cyclosporin A, has recently been shown to be identical with peptidyl prolyl cis–trans isomerase [Fischer, G., Wittmann-Liebold, B., Lang, K., Kiefhaber, T., & Schmid, F. X. (1989) *Nature 337*, 476; Takahashi, N., Hayano, T., & Suzuki, M. (1989) *Nature 337*, 473]. To provide a mechanistic framework for studies of the interaction of cyclophilin with cyclosporin, we investigated the mechanism of the PPI-catalyzed cis to trans isomerization of Suc-Ala-Xaa-*cis*-Pro-Phe-pNA (Xaa = Ala, Gly). Our mechanistic studies of peptidyl prolyl cis–trans isomerase include the determination of steady-state kinetic parameters, pH and temperature dependencies, and solvent and secondary deuterium isotope effects. The results of these experiments support a mechanism involving catalysis by distortion in which the enzyme uses free energy released from favorable, noncovalent interactions with the substrate to stabilize a transition state that is characterized by partial rotation about the C–N amide bond.

The recent finding (Fischer et al., 1989a; Takahashi et al., 1989) that cyclophilin and peptidyl prolyl cis–trans isomerase (PPI)[1] are identical and that cyclosporin A potently inhibits PPI raises the possibility of designing immunosupressive agents

0006-2960/90/0429-1684$02.50/0

on the basis of the inhibition of PPI. To rationally design these inhibitors, it will be essential to have a clear understanding of PPI's mechanism of action. Previous studies (Fischer et al., 1989a,b) of this enzyme's mechanism concluded that it involves the nucleophilic addition of an active site thiol to the carbonyl carbon of -Xaa-Pro-, to form a tetrahedral, hemithioorthoamide intermediate. According to this mechanism, formation of the intermediate is then followed by rotation about the C–N bond and, finally, collapse of the tetrahedral intermediate to liberate free enzyme and the isomerized -Xaa-Pro- peptide. This hypothesis is based on two findings (Fischer et al., 1989a,b): (1) *p*-(Hydroxymercuri)benzoate modifies an active site Cys residue with concomitant loss of enzyme activity. (2) An inverse secondary deuterium isotope effect is observed for k_c/K_m. That is, for -Gly(L,L)-Pro-, where L is H or D, $^Hk/^Dk < 1$.

To probe the mechanism of PPI in greater detail, we determined steady-state kinetic parameters, pH and temperature dependencies, and solvent and secondary deuterium isotope effects for reactions of this enzyme. Our results suggest a mechanism involving catalysis by distortion and are inconsistent with mechanisms involving the addition of an active-site nucleophile to the carbonyl carbon of -Xaa-Pro-.

Materials and Methods

General. Buffer salts and deuterium oxide were from Sigma Chemical Co. Water was distilled and passed through a deionizer. Buffers for the solvent isotope effect studies were prepared as described previously (Stein et al., 1983, 1987). Calf thymus PPI was kindly provided by Dr. John Siekierka (Immunology Department, Merck & Co.) as a 300 μg/mL (17 μM) solution in phosphate-buffered saline. This material was purified by the procedure of Harding et al. (1986).

Substrates. Suc-Ala-Ala-Pro-Phe-pNA was purchased from Sigma Chemical Co. Suc-Ala-Gly-Pro-Phe-pNA and Suc-Ala-Gly(D,D)-Pro-Phe-pNA were prepared by BACHEM (Switzerland). Fast-atom bombardment mass spectroscopy confirmed the molecular weight of the peptides. The peptides were >98% pure on the basis of HPLC and proton NMR. Isotopic labeling of the deuterated compound was >98% on the basis of proton NMR. "Kinetic purity" was established as outlined previously (Stein, 1988). Stock solutions (2.2 mM) of substrates were prepared in DMSO and diluted 30-fold into buffer to a concentration of 73 μM.

Assay for Prolyl Isomerization (Fischer et al., 1986). In typical kinetic experiments, 2.900 mL of a 70–75 μM stock solution of Suc-Ala-Xaa-Pro-Phe-pNA [Xaa = Ala, Gly, or Gly(D,D)] in buffer and 0 or 0.015 mL of a stock solution of PPI were added to a 4-mL disposable polystyrene cuvette, and the cuvette was placed in the jacketed cell holder of an Aviv Model 14DS spectrophotometer. Constant temperature was maintained within the cuvette by water circulated from a Brinkmann RM6 water bath and continuously monitored with an Omega thermistor thermometer that measured the temperature of the reaction cuvette. Temperature variation during a kinetic run was less than 0.02 °C. After the reaction solution had reached thermal equilibrium (≥15 min), we started the reaction by the addition of 0.100 mL of a 2.24 mM stock solution of CT in 1 mM HCl. Reaction progress was monitored by the absorbance change at 390 nm ($\Delta\epsilon$ = 13 400) that accompanies the hydrolysis of the anilide bond and the release of *p*-nitroaniline product. For each kinetic run, between 300

Scheme I: Assay for Prolyl Isomerization

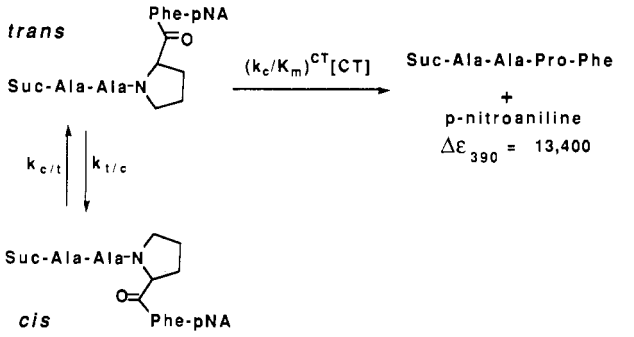

and 1000 data points, corresponding to {time, OD_{390}} pairs, were collected by an AT & T PC 6300 microcomputer interfaced to the spectrophotometer. Since these reactions were all conducted at a concentration of Suc-Ala-Xaa-*cis*-Pro-Phe-pNA much less than its K_m for PPI, the progress curves, after the initial rapid CT-catalyzed consumption of Suc-Ala-Xaa-*trans*-Pro-Phe-pNA, were first-order in substrate and could be fit to a simple first-order rate law. The analysis program was written by Dr. Phil Huskey (Chemistry Department, Rutgers University, Newark, NJ).

Results

Assay Method for Prolyl Isomerization and Analysis of Progress Curves. The assay that we use for PPI (Fischer et al., 1984) is a coupled assay and relies on chymotrypsin's inability to cleave peptide substrates with a *cis*-Pro at the P_2 position. This assay is illustrated in Scheme I for Suc-Ala-Ala-Pro-Phe-pNA, where $k_{t/c}$ and $k_{c/t}$ are first-order rate constants for nonenzymatic prolyl isomerization, $(k_c/K_m)^{CT}$ is the second-order rate constant for reaction of chymotrypsin with Suc-Ala-Ala-Pro-Phe-pNA, and $(k_c/K_m)^{CT}[CT]$ is the pseudo-first-order rate constant for the hydrolysis of substrate at a given chymotrypsin concentration. (In our kinetic expressions, the superscript associated with a rate constant identifies the enzyme.)

When a sufficiently high concentration of chymotrypsin reacts with an equilibrated solution of Suc-Ala-Ala-*cis*,-*trans*-Pro-Phe-pNA, Suc-Ala-Ala-*trans*-Pro-Phe-pNA will be entirely consumed before the cis–trans isomerization can reequilibrate. In such a situation, $(k_c/K_m)^{CT}[CT]$ is much greater than $k_{c/t}$, and the hydrolysis of the peptide will be rate-limited by $k_{c/t}$. The rate of *p*-nitroaniline production will equal $k_{c/t}$[Suc-Ala-Ala-*cis*-Pro-Phe-pNA], and progress curves for the accumulation of *p*-nitroaniline, after the burst of Suc-Ala-Ala-*trans*-Pro-Phe-pNA hydrolysis, will be first-order in Suc-Ala-Ala-*cis*-Pro-Phe-pNA with rate constant $k_{c/t}$.

When this assay is used to follow PPI-catalyzed prolyl isomerization, the observed first-order rate constant for cis isomerization, k_{obs}, will equal the sum $k_{c/t} + (k_c/K_m)^{PPI}[PPI]$. This assumes that the concentration of Suc-Ala-Ala-*cis*-Pro-Phe-pNA is less than its K_m for PPI. Given that $K_m > 10^{-2}$ M (see below), this condition is always met. In most assays, [PPI] is adjusted so that $k_{c/t}$ contributes 10% or less to k_{obs}.

This assay is illustrated by the progress curves of Figure 1A for the PPI-catalyzed prolyl isomerization of Suc-Ala-Gly-*cis*-Pro-Phe-pNA. In this figure, the total absorbance change is 1.08. The first 88% of this change occurs in less than 8 s and reflects the rapid reaction of Suc-Ala-Gly-*trans*-Pro-Phe-pNA with chymotrypsin. The remaining 12% of the substrate is Suc-Ala-Gly-*cis*-Pro-Phe-pNA and cannot react with chymotrypsin. The first-order PPI-catalyzed conversion of Suc-Ala-Gly-*cis*-Pro-Phe-pNA to Suc-Ala-Gly-*trans*-Pro-Phe-pNA rate limits the reaction of Suc-Ala-Gly-*trans*-Pro-

[1] Abbreviations: CT, α-chymotrypsin; PPI, peptidyl prolyl cis–trans isomerase; Suc-Ala-Ala-Pro-Phe-pNA, *N*-succinyl-Ala-Ala-Pro-Phe-*p*-nitroanilide; eu, entropy unit [cal/(mol·K)].

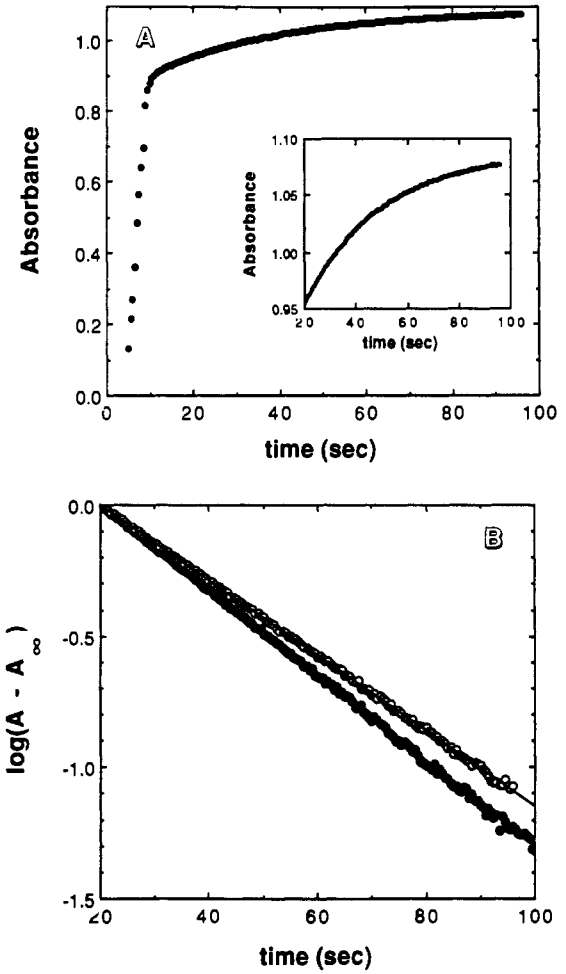

FIGURE 1: (A) Progress curve for the hydrolysis of Suc-Ala-Gly-Pro-Phe-pNA by chymotrypsin in the presence of PPI. The data were collected at pH 7.8 in a buffered solution containing 50 mM HEPES. Final concentrations in the reaction solution: [CT] = 74 μM; [PPI] = 33 nM; [Suc-Ala-Gly-Pro-Phe-pNA] = 71 μM. Temperature = 10 °C. Inset: The data of this inset consist of roughly 300 pairs of {time, OD_{390}} data points that were taken from the high-absorbance region of the main figure and reflect the first-order cis to trans isomerization of Suc-Ala-*cis*-Gly-Pro-Phe-pNA. (B) Logarithmic, linear transform of the data of (A). This figure demonstrates that the PPI-catalyzed cis to trans isomerization of Suc-Ala-*cis*-Gly-Pro-Phe-pNA adheres to a first-order rate law for at least five half-times (>95% reaction). The closed and open circles reflect the isomerization of Suc-Ala-*cis*-Gly(D,D)-Pro-Phe-pNA and Suc-Ala-*cis*-Gly-Pro-Phe-pNA, respectively.

Phe-pNA with chymotrypsin and is reflected in the progress curve of the inset of Figure 1A. The absorbance change seen here is only about 0.12 but is sufficiently large to allow the collection of reliable kinetic data. This progress curve is composed of about 300 data points and follows strict first-order kinetics for at least 95% of the reaction (Figure 1B).

To accurately determine first-order rate constants for prolyl isomerization, it is essential that none of the data reflecting the initial burst of Suc-Ala-Xaa-*trans*-Pro-Phe-pNA hydrolysis be used in the progress curve analyses. We were able to meet this requirement by following an iterative analysis procedure. For each successive analysis in this procedure, we constrained the point at time zero to be a point that occurred later on the progress curve. Analyses that contained data points from the burst phase would invariably give poor nonlinear regression fits that were characterized by large sums-of-squares-of-residual terms and rate constants with large standard deviations. With each successive iteration, less and less of the burst phase was included in the analysis, and the fits became progressively

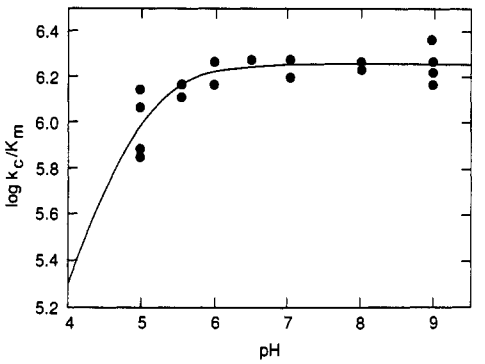

FIGURE 2: pH dependence of k_c/K_m for the PPI-catalyzed prolyl isomerization of Suc-Ala-Ala-*cis*-Pro-Phe-pNA. Reactions were conducted over a pH range of 5–9 in buffered solutions containing 50 mM sodium acetate (pH 5), 50 mM MES (5.5 ≤ pH ≤ 6.5), 50 mM HEPES (7.0 ≤ pH ≤ 8.0), and 50 mM CHES (pH 9.0). Final concentrations in reaction solutions: [CT] = 74 μM; [Suc-Ala-Ala-Pro-Phe-pNA] = 71 M; [PPI] = 15 nM. Temperature = 10 °C. Data were fit to $(k_c/K_m)_{obs} = (k_c/K_m)_{limit}/(1 + [H^+]/K_a)$ to obtain the best-fit parameters, $(k_c/K_m)_{limit} = (1.81 \pm 0.06) \times 10^6$ M^{-1} s^{-1} and $pK_a = 4.92 \pm 0.09$.

better until no further improvement was attained. We used the rate constants that were generated from fitting these latter progress curves.

Steady-State Kinetic Parameters for Reactions of PPI. k_c/K_m for the PPI-catalyzed isomerization of Suc-Ala-Ala-*cis*-Pro-Phe-pNA at pH 7.8 and 10 °C is 2×10^6 M^{-1} s^{-1} (Figure 1A). The K_m for this reaction has been estimated to be greater than 10^{-3} M (Fischer et al., 1989b). To obtain a better estimate of K_m, we attempted to determine K_i values for several proline-containing peptides, including Ala-Pro, Ala-Pro-Phe, Ala-Pro-Gly, Ala-Ala-Pro-Ala, and Ala-Ala-Pro-Ala-Ala. Since these peptides should act as alternate substrate inhibitors of PPI, their K_i values can be interpreted as K_m values. In these experiments, we determined first-order rate constants for the PPI-catalyzed isomerization of Suc-Ala-Ala-*cis*-Pro-Phe-pNA in the presence of 5 mM peptide. In all cases, inhibition was less than 10% (data not shown). This lack of inhibition at 5 mM peptide is consistent with a very high K_m for PPI and allows us to place a conservative lower limit on K_i, and thus K_m, of 2×10^{-2} M. With $K_m \geq 2 \times 10^{-2}$ M and an observed value of k_c/K_m of 2×10^6 M^{-1} s^{-1}, we can now calculate $k_c \geq 4 \times 10^4$ s^{-1}.

pH Dependence of PPI Catalysis. k_c/K_m for the PPI-catalyzed isomerization of Suc-Ala-Ala-*cis*-Pro-Phe-pNA is independent of pH between 5.5 and 9 (Figure 2) and shows a modest decrease in magnitude below pH 5.5. When the data are fit by nonlinear least squares to a simple protonation model, a best-fit pK_a of 4.9 ± 0.1 is found.

Temperature Dependence of PPI Catalysis. Activation parameters were determined for the prolyl isomerization of Suc-Ala-Ala-*cis*-Pro- Phe-pNA from Eyring plots (Figure 3) of ln $[k(h/k^*T)]$ vs $1/T$, where h is Planck's constant, k^* is Boltzmann's constant, and T is expressed in Kelvin. k corresponds either to the nonenzymatic first-order rate constant or to $(k_c/K_m)[PPI]_{standard\text{-}state}$, where a standard-state enzyme concentration of 10^{-6} M was chosen. From these plots, the enthalpy of activation is obtained from the slope, $-\Delta H^*/R$, and the entropy of activation from the y intercept, $\Delta S^*/R$, where R is the gas constant. For the nonenzymatic reaction, ΔH^* and ΔS^* equal 20.3 ± 0.2 kcal/mol and 3.5 ± 0.6 eu, respectively, while for the PPI-catalyzed reaction ΔH^* and ΔS^* equal 3.87 ± 0.04 kcal/mol and −44 ± 1 eu, respectively.

Solvent Deuterium Isotope Effects. Rate constants were determined in buffered solutions of light and heavy water for

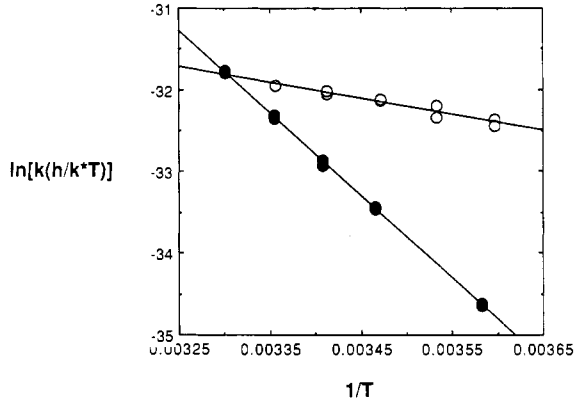

FIGURE 3: Eyring plots for the enzymatic and nonenzymatic prolyl isomerization of Suc-Ala-Ala-*cis*-Pro-Phe-pNA. Nonenzymatic reaction, filled circles; PPI-catalyzed reaction, open circles. The data were collected at pH 7.8 in a buffered solution containing 50 mM HEPES. Final concentrations: (in reaction solutions) [CT] = 74 μM and [Suc-Ala-Ala-Pro-Phe-pNA] = 71 μM; (in the enzyme-catalyzed reaction) [PPI] = 33 nM.

the uncatalyzed and PPI-catalyzed cis-to-trans isomerization of Suc-Ala-Ala-*cis*-Pro-Phe-pNA. The solvent isotope effect, $^{H_2O}(k_c/K_m)/^{D_2O}(k_c/K_m)$, was calculated according to eq 1,

$$^{H_2O}(k_c/K_m)/^{D_2O}(k_c/K_m) = (^{H_2O}k_{obs} - {}^{H_2O}k_u)/(^{D_2O}k_{obs} - {}^{D_2O}k_u) \quad (1)$$

where $^{H_2O}k_{obs}$ and $^{D_2O}k_{obs}$ are the observed first-order rate constants for isomerization of Suc-Ala-Ala-*cis*-Pro-Phe-pNA in H_2O and D_2O, respectively, in the presence of PPI and $^{H_2O}k_u$ and $^{D_2O}k_u$ are the first-order rate constants for the uncatalyzed isomerization of Suc-Ala-Ala-*cis*-Pro-Phe-pNA in H_2O and D_2O, respectively. Rate constants were determined as outlined under Materials and Methods. For the uncatalyzed reaction, the isotope effects were calculated directly as the ratio $^{H_2O}k_u/^{D_2O}k_u$. Three replicate determinations yielded the means and standard deviations: $^{H_2O}k_u/^{D_2O}k_u = 1.07 \pm 0.01$ and $^{H_2O}(k_c/K_m)/^{D_2O}(k_c/K_m) = 0.98 \pm 0.08$.

Secondary Deuterium Isotope Effect Determinations. Isotope effects for uncatalyzed and calf thymus PPI-catalyzed prolyl isomerization at 10 °C were determined on three separate occasions. Each of the three experiments involved five individual isotope effect determinations. Each of these individual isotope effect determinations was calculated according to

$$^{H}(k_c/K_m)/^{D}(k_c/K_m) = (^{H}k_{obs} - {}^{H}k_u)/(^{D}k_{obs} - {}^{D}k_u) \quad (2)$$

where $^{H}k_{obs}$ and $^{D}k_{obs}$ are the observed first-order rate constants for isomerization of the protium- and deuterium-labeled substrates in the presence of PPI and $^{H}k_u$ and $^{D}k_u$ are the first-order rate constants for uncatalyzed isomerization of the protium- and deuterium-labeled substrates. Rate constants were determined as outlined under Materials and Methods. For the uncatalyzed reaction, the isotope effect for each determination was calculated directly as the ratio $^{H}k_u/^{D}k_u$.

For each of the three experiments, five isotope effect determinations for the uncatalyzed and catalyzed reactions were used to calculate the means and standard deviations of Table I. The two overall isotope effects that we report, $^{H}k_u/^{D}k_u = 1.056 \pm 0.018$ and $^{H}(k_c/K_m)/^{D}(k_c/K_m) = 1.132 \pm 0.012$, are the means and standard deviations of the four means (Sokal & Rohlf, 1981) for the uncatalyzed and PPI-catalyzed reactions, respectively.

Experiment 4 of Table I was performed at a substrate concentration 3 times less than the concentration used in experiments 1–3. That the same isotope effect was found demonstrates the "kinetic purity" of the two substrates. That is, the substrates contained no inhibitors or activators of PPI that could compromise our isotope effect measurements. In addition, experiment 4 was peformed with PPI from porcine kidney.

Table I: Secondary Deuterium Isotope Effects for the Nonenzymatic and PPI-Catalyzed Cis to Trans Isomerization of Suc-Ala-Gly-*cis*-Pro-Phe-pNA

expt	temp (°C)	PPI source	$^{H}k_u/^{D}k_u$	$^{H}(k_c/K_m)/^{D}(k_c/K_m)$
1[a]	10	calf thymus	1.037 ± 0.020	1.120 ± 0.048
2[a]	10	calf thymus	1.072 ± 0.019	1.132 ± 0.030
3[a]	10	calf thymus	1.057 ± 0.033	1.143 ± 0.038
			1.056 ± 0.018	1.132 ± 0.012
4[b]	10	porcine kidney	1.035 ± 0.016	1.133 ± 0.008
5[c]	2	porcine kidney		1.138 ± 0.024

[a] The data were collected at pH 7.8 in a buffered solution containing 50 mM HEPES. Final concentrations: (in reaction solutions) [CT] = 74 μM and [Suc-Ala-Ala-Pro-Phe-pNA] = 71 μM; (in the enzyme-catalyzed reaction) [PPI] = 33 nM. [b] Same experimental conditions as described in footnote *a* but [S] = 25 μM. [c] Reactions started by the addition of substrate to a thermally equilibrated solution of CT and PPI, according to the method of Fischer et al. (1989b).

Table II: Summary of Results from Mechanistic Studies of PPI-Catalyzed and Nonenzymatic Prolyl Isomerization

mechanistic probe	PPI catalyzed	uncatalyzed
steady-state kinetics[a,b]	$k_c/K_m = 2 \times 10^6$ M^{-1} s^{-1} $k_c \geq 4 \times 10^4$ s^{-1} $K_m \geq 2 \times 10^{-2}$ M	$k = 8.6 \times 10^{-3}$ s^{-1}
pH dependence[b,c]	$pK_a = 4.92 \pm 0.09$	none
temperature dependence[b,d]	$\Delta H^* = 4$ kcal/mol $-T\Delta S^* = 13$ kcal/mol	$\Delta H^* = 20$ kcal/mol $-T\Delta S^* = -1$ kcal/mol
solvent isotope effect[a,b]	0.98 ± 0.08	1.07 ± 0.01
secondary isotope effect[a,e]	1.13 ± 0.01	1.05 ± 0.02

[a] 10 °C, pH 7.8. [b] Substrate: Suc-Ala-Ala-Pro-Phe-pNA. [c] 10 °C. [d] pH 7.8; $[PPI]_{standard\text{-}state} = 10^{-6}$ M. [e] Substrate: Suc-Ala-Gly-Pro-Phe-pNA.

Experiment 5 was performed according to the method of Fischer (1987b) in which reactions were conducted at 2.0 °C and started by the addition of substrate to a solution of PPI and chymotrypsin. In this experiment, the substrate was prepared in DMSO, while Fischer (1987b) prepared substrate solutions in ethanol. In our hands, isotope effect determinations using substrates prepared in ethanol resulted in large normal effects, but with standard deviations that were greater than 20% (data not shown). Although we have not determined the origin of the lack of precision when ethanol is the vehicle for the substrate, we suspect that it might be related to solubility of the peptide.

Discussion

In this study of the mechanism of PPI, not only did we want to characterize structural features of the rate-limiting[2] transition state, but more specifically, we wanted to address the issue of nucleophilic catalysis. To this end, we employed five

[2] As O'Leary (1989) has recently pointed out, there is no generally agreed upon definition for the term "rate-determining" or "rate-limiting" step (Cleland, 1975; Northrop, 1981; Ray, 1983). In this paper, we are primarily concerned with elucidating structural features of the "rate-limiting transition state" for the enzymic process that is governed by the steady-state kinetic term k_c/K_m. In this paper, rate-limiting transition state will refer to the transition state of highest free energy, and by analogy, rate-limiting step will refer to that reaction step which has the highest free energy. Where several transition states have similar free energies, these steps will be said to be "partially rate limiting".

probes of mechanism and transition-state structure: steady-state kinetics, pH and temperature dependencies, and solvent and secondary deuterium isotope effects. Taken together, the results of this study, summarized in Table II, do not support a mechanism involving nucleophilic catalysis. In this section, we will discuss the individual findings of this study and then go on to suggest an alternate mechanism for PPI involving catalysis by distortion.

First, the steady-state kinetic parameters that we determined for the PPI-catalyzed isomerization of Suc-Ala-Ala-*cis*-Pro-Phe-pNA are unusually large: k_c/K_m (2×10^6 M^{-1} s^{-1}) approaches the second-order rate constant of 10^7 M^{-1} s^{-1} for association of a protein and small peptide (Fersht, 1985; Gutfreund, 1972), while our estimate of k_c ($>4 \times 10^4$ s^{-1}) is an order of magnitude faster than acylation of chymotrypsin by the activated ester Ac-Trp-*p*-nitrophenyl ester (Hirohara et al., 1977), a rate constant that is at the upper limit of rate constants for acid-base catalysis (10^3–10^4 s^{-1}). These rate constants for PPI are even more remarkable when we consider that Suc-Ala-Ala-Pro-Phe-pNA was chosen simply for convenience of assay and not because of a strict specificity requirement. The mechanistic significance of the rate constants becomes clear if we compare them to kinetic parameters determined for thiol protease catalyzed peptide hydrolysis (Bromme et al., 1987). For these reactions, both k_c and k_c/K_m reflect a transition state that has partial sp^3 character; that is, the transition state that is reflected by these rate constants precedes the tetrahedral intermediate that occurs along the reaction pathway to the acyl-enzyme. This is identical to the intermediate and transition state that has been proposed for PPI (Fischer et al., 1987a,b). Now, k_c/K_m for peptide hydrolysis by thiol proteases ranges from 10^2 to 10^4 M^{-1} s^{-1}, while k_c ranges from 1 to 100 s^{-1}. The corresponding values that we observe for PPI are several orders of magnitude larger than these and therefore are inconsistent with mechanisms involving thiol attack on a peptide bond.

Second, k_c/K_m for PPI is independent of pH over a broad range of pH and, indeed, over the range of pH where most enzyme active site nucleophiles (e.g., His, Ser, Cys, Lys) normally ionize. Although the pK_a of 4.9 that we estimate for the active site of PPI is consistent with ionization of a carboxylic acid moiety, examples of enzymic nucleophilic catalysis by an active-site carboxylate are rare and, in fact, nonexistent for attack on a peptide bond. For PPI, a pK_a of 5 suggests that a thiol is not part of the catalytic machinery of this enzyme since thiol moieties typically have pK_a values around 9 (Tipton & Dixon, 1979).

Third, the activation parameters for PPI catalysis also suggest a unique mechanism, one not involving nucleophilic catalysis. The small enthalpy of activation ($\Delta H^\ddagger$ = 3.9 kcal/mol) and the large, negative entropy of activation ($-T\Delta S^\ddagger$ = 13.2 kcal/mol; T = 300 K) suggest rate limitation by a physical process rather than by a covalent, chemical reaction (Acheson et al., 1987). If nucleophilic attack were rate limiting, we would expect a much larger enthalpy of activation and possibly a less negative entropy of activation.

Fourth, the solvent isotope effect of unity that we observe is inconsistent with a reaction mechanism involving rate-limiting, general base catalyzed nucleophilic attack, since such a mechanism would produce a large, normal solvent isotope effect between 1.5 and 4 (Schowen, 1978). This value is also inconsistent with a catalytically important thiol, since solvent isotope effects accompanying thiol participation are expected to be around 0.57 (Schowen, 1978). However, a solvent isotope effect of unity does not exclude nucleophilic participation by the thiolate anion. This, of course, requires not only that the thiol have a low pK_a but also that PPI binds the substrate only when the active-site thiol is ionized.

Finally, the most compelling evidence against the participation of an active site nucleophile during catalysis by PPI is the normal secondary deuterium isotope effect of 1.13 that we observe for the isomerization of Suc-Ala-Gly-*cis*-Pro-Phe-pNA. If nucleophilic attack at the carbonyl carbon of the Gly–Pro bond were involved and rate limiting, an inverse isotope effect would have been observed (Kovach et al., 1980; Hogg et al., 1980). Typically, secondary deuterium isotope effects for nucleophilic attack at Gly amides or esters range from 0.92 to 0.96 (Stein et al., 1983; Stein, 1988). These values arise from the loss of hyperconjugation and tightening of force constants associated with the Gly hydrogens that occur as the substrate proceeds from an sp^2-hybridized ground state to an sp^3-hybridized, tetrahedral-intermediate-like transition state. In contrast, the isotope effect of 1.13 for PPI-catalyzed isomerization indicates that, in the transition state for this reaction, hyperconjugation from the Gly hydrogens is enhanced, and force constants are loosened, relative to the ground state. This can be explained if the transition state is characterized by partial rotation about the Gly–Pro amide bond. In this transition state, the resonance stabilization of the ground state no longer exists, and the carbonyl C=O bond now resembles a ketone in its ability to hyperconjugate with the Gly hydrogens. Hyperconjugation in this transition state is greater than in the resonance-stabilized amide ground state.

In summary, the results of this study (Table II) are clearly inconsistent with a mechanism involving nucleophilic catalysis by an active-site thiol. While the results reported by Fischer et al. (1989a) demonstrate that modification of a thiol destroys enzymic activity, they do not demonstrate that the thiol is part of the enzyme's catalytic apparatus. For example, if this thiol were important for PPI's structural integrity, its modification could be accompanied by an alteration of the protein's three-dimensional structure resulting in a loss of activity. What we find disturbing is the disagreement between the normal isotope effect that we report here and the inverse isotope effect that is reported by Fischer et al. (1989b). This discrepancy cannot be attributed to either differences in experimental conditions or enzyme identity, since we obtain an isotope effect of 1.14 (Table I, experiment 5) when we reproduce the experimental conditions reported by Fischer et al. (1989b). We also confirmed the chemical, isotopic, and "kinetic" purity (Stein, 1988) of our peptide substrates (Table I, experiment 4).

Taken together, our results support a mechanism involving catalysis by distortion in which PPI binds and stabilizes a transition state that is characterized by partial rotation about the C–N amide bond. The energy that is required to distort this bond out of planarity with the C=O bond, thereby destroying the resonance stabilization of the amide linkage, is supplied by favorable transition-state binding interactions between enzyme and substrate (Jencks, 1975). The energetic cost for -Ala–Pro- bond distortion is reflected in the large entropy of activation ($-T\Delta S^\ddagger$ = 13.2 kcal/mol at 300 K) that is required to distort and constrain the substrate to a conformation that allows optimal interaction with the enzyme. Once the entropic bill has been paid, the reaction occurs with little enthalpic cost ($\Delta H^\ddagger$ = 3.9 kcal/mol). This mechanism is unique in enzymology. PPI appears to use none of the catalytic "devices" that enzymes typically employ (e.g., general-acid/general-base or nucleophilic catalysis; Jencks, 1969) but rather utilizes intrinsic binding energy that is available

from substrate–enzyme interactions to stabilize the catalytic transition state (Jencks, 1975). It is our hope that these and other mechanistic studies of PPI will provide the basis for the rational design of therapeutically useful inhibitors of this important enzyme.

References

Acheson, S. A., Barlow, P. N., Lee, G. C., Swanson, M. L., & Quinn, D. M. (1987) *J. Am. Chem. Soc. 109*, 246–252.

Bromme, D., Bescherer, K., Kirschke, H., & Fittkau, S. (1987) *Biochem. J. 245*, 381–385.

Cleland, W. W. (1975) *Acc. Chem. Res. 8*, 145–151.

Fersht, A. (1985) *Enzyme Structure and Mechanism*, pp 147–153, W. H. Freeman, New York.

Fischer, G., Bang, H., & Mech, C. (1984) *Biomed. Biochim. Acta 43*, 1101–1111.

Fischer, G., Berger, E., & Bang, H. (1989a) *FEBS Lett. 250*, 267–270.

Fischer, G., Wittmann-Liebold, B., Lang, K., Kiefhaber, T., & Schmid, F. X. (1989b) *Nature 337*, 476–478.

Gutfreund, H. (1972) *Enzymes: Physical Principles*, p 159, Wiley, New York.

Handschumacher, R. E., Harding, M. W., Rice, J., Drugge, R. J., & Speicher, D. W. (1984) *Science 226*, 544–547.

Harding, M. W., Handschumacher, R. E., & Speicher, D. W. (1986) *J. Biol. Chem. 261*, 8547–8555.

Hirohara, H., Philipp, M., & Bender, M. L. (1977) *Biochemistry 16*, 1573–1580.

Hogg, J. L., Rodgers, J., Kovach, I. M., & Schowen, R. L. (1980) *J. Am. Chem. Soc. 102*, 79–85.

Jencks, W. P. (1969) *Catalysis in Chemistry and Enzymology*, McGraw-Hill, New York.

Jencks, W. P. (1975) *Adv. Enzymol. 43*, 219–404.

Kovach, I. M., Hogg, J. L., Raben, T., Halbert, K., Rodgers, J., & Schowen, R. L. (1980) *J. Am. Chem. Soc. 102*, 1991–1999.

Northrop, D. B. (1981) *Annu. Rev. Biochem. 50*, 103–131.

Ray, W. J. (1983) *Biochemistry 22*, 4625–4637.

Schowen, K. B. (1978) in *Transition States of Biochemical Processes* (Gandour, R. D., & Schowen, R. L., Eds.) p 225, Plenum Press, New York.

Sokal, R. R., & Rohlf, F. J. (1981) *Biometry*, 2nd ed., pp 128–137, W. H. Freeman, New York.

Stein, R. L. (1988) *J. Am. Chem. Soc. 110*, 7907–7908.

Stein, R. L., Elrod, J. P., & Schowen, R. L. (1983) *J. Am. Chem. Soc. 105*, 2446–2452.

Stein, R. L., Strimpler, A. M., Hori, H., & Powers, J. C. (1987) *Biochemistry 26*, 1305–1314.

Takahashi, N., Hayano, T., & Suzuki, M. (1989) *Nature 337*, 473–475.

Tipton, K. F., & Dixon, H. B. F. (1979) *Methods Enzymol. 63*, 183–234.

Three-Dimensional Structure of Interleukin 8 in Solution†

G. Marius Clore,*,‡ Ettore Appella,§ Masaki Yamada,∥ Kouji Matsushima,⊥ and Angela M. Gronenborn*,‡

Laboratory of Chemical Physics, National Institute of Diabetes and Digestive and Kidney Diseases, and Laboratory of Cell Biology, National Cancer Institute, National Institutes of Health, Bethesda, Maryland 20892, Laboratory of Molecular Immunoregulation, Biological Response Modifiers Program, Division of Cancer Treatment, National Cancer Institute, Frederick, Maryland 21701-1013, and Research Laboratories, Dainippon Pharmaceutical Company, Suita, Osaka 564, Japan

Received November 27, 1989; Revised Manuscript Received December 20, 1989

ABSTRACT: The solution structure of the interleukin 8 (IL-8) dimer has been solved by nuclear magnetic resonance (NMR) spectroscopy and hybrid distance geometry–dynamical simulated annealing calculations. The structure determination is based on a total of 1880 experimental distance restraints (of which 82 are intersubunit) and 362 torsion angle restraints (comprising ϕ, ψ, and χ_1 torsion angles). A total of 30 simulated annealing structures were calculated, and the atomic rms distribution about the mean coordinate positions (excluding residues 1–5 of each subunit) is 0.41 ± 0.08 Å for the backbone atoms and 0.90 ± 0.08 Å for all atoms. The three-dimensional solution structure of the IL-8 dimer reveals a structural motif in which two symmetry-related antiparallel α-helices, approximately 24 Å long and separated by about 14 Å, lie on top of a six-stranded antiparallel β-sheet platform derived from two three-stranded Greek keys, one from each monomer unit. The general architecture is similar to that of the $\alpha 1/\alpha 2$ domains of the human class I histocompatibility antigen HLA-A2. It is suggested that the two α-helices form the binding site for the cellular receptor and that the specificity of IL-8, as well as that of a number of related proteins involved in cell-specific chemotaxis, mediation of cell growth, and the inflammatory response, is achieved by the distinct distribution of charged and polar residues at the surface of the helices.

Communication between different cells of the immune system is achieved in part by a complex cascade of interacting proteins known as cytokines. The subject of the present study is the cytokine interleukin 8 (IL-8)[1] [for a review, see Matsushima and Oppenheim (1989)], also known variously as

† This work was supported by the Intramural AIDS Targeted Antiviral Program of the Office of the Director of the National Institutes of Health (G.M.C. and A.M.G.).

‡ Laboratory of Chemical Physics, NIDDKD, NIH.

§ Laboratory of Cell Biology, NCI, NIH.

∥ Laboratory of Molecular Immunoregulation, National Cancer Institute.

⊥ Research Laboratories, Dainippon Pharmaceutical Co.

[1] Abbreviations: IL-8, interleukin 8; MCAF, monocyte chemotactic and activating factor; PF4, platelet factor 4; GRO, growth-related gene product; MGSA, melanoma growth stimulating activity; γIP-10, γ-interferon-induced protein; βTG, β-thromboglobulin; 9E3, chicken Rous sarcoma virus inducible protein; MHC, major histocompatibility complex; NOE, nuclear Overhauser effect; NOESY, two-dimensional nuclear Overhauser enhancement spectroscopy; PE-COSY, primitive exclusive two-dimensional correlated spectroscopy; SA, simulated annealing.

0006-2960/90/0429-1689$02.50/0